Journal of Hazardous Materials 213–214 (2012) 258–264

Contents lists available at SciVerse ScienceDirect

Journal of Hazardous Materials

journal homepage: www.elsevier.com/locate/jhazmat

High-strength hydrogel as a reusable adsorbent of copper ions

Ning Wang, Yanjiao Han, Yuan Liu, Tao Bai, Han Gao, Peng Zhang, Wei Wang*, Wenguang Liu*

School of Materials Science and Engineering, Tianjin Key Laboratory of Composite and Functional Materials, Tianjin University, Tianjin 300072, PR China

ARTICLE INFO

Article history:
Received 7 September 2011
Received in revised form 16 January 2012
Accepted 27 January 2012
Available online 6 February 2012

Keywords:
High-strength hydrogel
Copper ion
Adsorption
Reusability

ABSTRACT

A mechanically strong hydrogel was prepared by photoinitiated polymerization of oligo(ethylene glycol) methacrylate (OEGMA), 2-vinyl-4,6-diamino-1,3,5-triazine (VDT) and cross-linker N,N′-methylenebisacrylamide (MBAA). Introduction of the monomer VDT considerably strengthened the mechanical properties of the hydrogel by self-hydrogen bonding of diaminotriazine, and enhanced the adsorption of copper ion onto the hydrogel by chelation between amino groups and metal ion. Adsorption studies were carried out by varying the OEGMA/VDT ratio, contact time, pH value, counterion and initial concentration of Cu^{2+} ions. The evaluation of adsorption properties showed that the hydrogel exhibited better correlation with Langmuir isotherm model. This adsorbent could be used repeatedly with little loss in adsorption capacity.

1. Introduction

Copper ion contamination in water resources has become an important issue of great concern due to the toxic effect on the human beings and even the entire ecological environment. Accumulation of Cu^{2+} in human body causes brain, skin, pancreas and heart diseases [1]. Hence, it is imperative to remove copper from water resource before discharging to the environment.

Several kinds of strategies have been attempted to remove heavy metal ions, such as ion exchange, membrane separation, reverse osmosis, chemical precipitation and adsorption [2–5]. Among the methods currently reported, adsorption technology has been proved to be one of the most effective and economic ways due to its easiness to operate and simplicity to design [1,7–9]. A variety of polymeric adsorbents have been investigated for copper adsorption, including polymer fibers [10,11], resins [12–14], nanocomposites [15,16], natural materials [17–19]. Recently, hydrogel-based sorbents functionalized with amino, hydroxyl, carboxyl, imidazole and hydrazine groups were reported to demonstrate high capacities in removal of metal ions from aqueous solutions due to their complexing abilities [20–22]. The main advantages of hydrogel-based adsorbents are easy loading, capturing of cations with simple chemicals in most cases, reusability and the possibility of semi-continuous operation [21]. Besides, high swelling and wettability can facilitate adsorption of target metals because the swelling of the three-dimensional networks is likely to give high specific surface area and more functional groups exposed are readily approachable for adsorption [23]; while the coordination resins, which are poorly swollen in water, limit the mobility of the functional groups [24]. The chemical stabilities of hydrogels, especially hydrolytic and thermal stabilities, make them very promising in the field of water purification [22,25]. Ali et al. prepared poly(vinylpyrrolidone/acrylic acid) (PVP/AAc) copolymer hydrogels that were shown to remove Cu^{2+} from aqueous solution with the maximum adsorption capacity of 0.36 mmol/g [22]. Cavus et al. investigated non-competitive removal of metal ions by poly(acrylic acid-co-methacrylamide) gels and found that the maximum adsorption capacity of the hydrogels was 0.64 mmol Cu^{2+}/g dry hydrogel [26]. Except for limited adsorption capacity, there are some other drawbacks seriously hindering the actual applications of hydrogels in metal ion removal such as lacking in reusability and poor mechanical strength caused by highly swollen network. So it is necessary to develop hydrogel-based adsorbents that are robust enough to withstand multiple handling and can release adsorbed metal ions in response to external stimuli and re-adsorb them repeatedly with little loss in mechanical properties.

The aim of this work is to synthesize a high-strength hydrogel which can adsorb Cu^{2+} ions effectively and be used repeatedly without loss in adsorption capacity and mechanical property. For this purpose, we synthesized 2-vinyl-4,6-diamino-1,3,5-triazine/oligo(ethylene glycol) methacrylate copolymer P(OEGMA-co-VDT) hydrogel by photo polymerization. The mechanical strength of hydrogels was tested and adsorption of Cu^{2+} ions onto

Abbreviations: P(OEGMA-co-VDT), copolymer hydrogel synthesized from OEGMA and VDT; POVx-y, P(OEGMA-co-VDT) hydrogel with weight ratio of OEGMA/VDT (x/y). e.g. POV2-3; cr-PVDT, crosslinked PVDT hydrogel; cr-POEGMA, crosslinked POEGMA hydrogel.

* Corresponding authors. Tel.: +86 22 27402487; fax: +86 22 27404724.
E-mail addresses: wwgfz@tju.edu.cn (W. Wang), wgliu@tju.edu.cn (W. Liu).

0304-3894/$ – see front matter © 2012 Elsevier B.V. All rights reserved.
doi:10.1016/j.jhazmat.2012.01.092

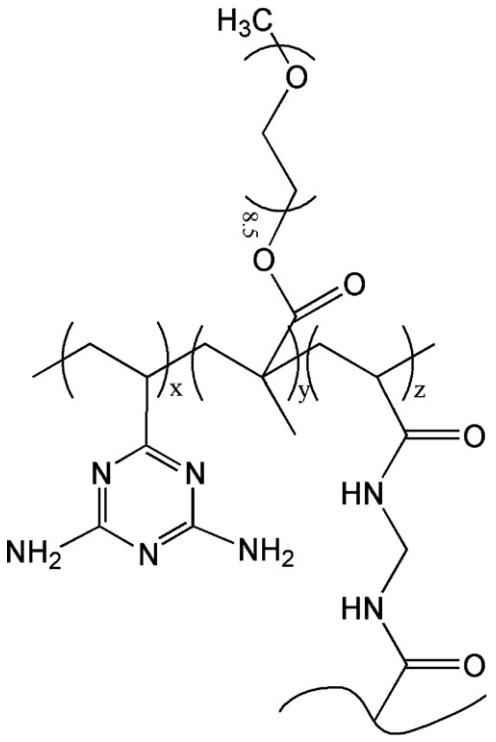

Fig. 1. Schematic molecular structure of P(OEGMA-co-VDT) hydrogel.

the hydrogels under different conditions (contact time, initial pH and concentration of Cu^{2+} solution and so on) was investigated. Furthermore, the reusable property of hydrogels was evaluated by repeated adsorption.

2. Experimental

2.1. Materials

2-Vinyl-4,6-diamino-1,3,5-triazine (VDT) was obtained from Tokyo Kasei Kogyo, and used as received. Oligo(ethylene glycol) methacrylate (OEGMA, 99%) and the initiator 2-hydroxy-4-(2-hydroxyethoxy)-2-methyl-propiophenone (IRGACURE-2959, 98%) were purchased from Sigma Aldrich. The cross-linker N,N′-methylenebisacrylamide (MBAA, 99%) and copper(II) perchlorate hexahydrate (99%) were provided by Johnson Matthey. Copper sulfate, copper nitrate and copper chloride obtained from Tianjin Guangfu Fine Chemical Research Institute were all analytical grades.

2.2. Synthesis of P(OEGMA-co-VDT) hydrogels

P(OEGMA-co-VDT) hydrogels were prepared by radical copolymerization of OEGMA and VDT in dimethyl sulfoxide (DMSO) in the presence of N,N′-methylenebisacrylamide (MBAA) as a cross-linking agent and 2-hydroxy-4-(2-hydroxyethoxy)-2-methyl-propiophenone (IRGACURE-2959) as an initiator. Initial monomer concentration in feed was kept constant at 10 wt%. The weight ratio of monomer, cross-linker and initiator was 5:1:0.12. A series of P(OEGMA-co-VDT) hydrogels whose schematic molecular structure is depicted in Fig. 1 were obtained by varying monomer feed ratio (Table S1). The reaction mixture was injected into plastic molds. The molds were then irradiated in a crosslink oven (XL-1000 UV Crosslinker, Spectronics Corporation, NY, USA) for 30 min. The resultant hydrogels were purified by immersing in distilled water, which was refreshed daily, for one week to remove reagent residues completely. Herein, POVx-y stands for P(OEGMA-co-VDT) hydrogel with weight ratio of OEGMA/VDT (x/y). In this study, crosslinked POEGMA (cr-POEGMA) and crosslinked PVDT (cr-PVDT) were synthesized in the same way.

2.3. Characterization of hydrogels

Attenuated total reflection Fourier transform infrared spectroscopy (ATR-FTIR) spectra of lyophilized hydrogel slices (0.2 mm in thickness) were recorded by Nicolet 380 FTIR spectrometer (USA) in a wavenumber range from 4000 to 400 cm^{-1} at a resolution of 0.5 cm^{-1}. Ge horizontal crystal (45° angle of incidence) was used for the samples.

2.4. Measurement of mechanical properties

The mechanical properties of hydrogels were measured on WDW-05 electromechanical tester (Time Group Inc., China) at room temperature. Swelling hydrogel strips (20 mm length, 6 mm width and 0.8 mm thickness) were used for tensile test. For compression tests, the samples were cut into cylinders (6.5 mm in diameter and 9 mm thick) and measured at the same tester. In both tests, crosshead speed was set at 10 mm/min, and three specimens were tested for each hydrogel sample.

2.5. Cu^{2+} adsorption

The stock solution of Cu^{2+} was prepared by dissolving copper perchlorate in distilled water. A thin circular slice of swollen hydrogel (9 mm in diameter and 0.2 mm thickness), with dry weight of 13 mg, was placed in a centrifuge tube containing 1 mL solution of Cu^{2+} ions with a certain concentration. The adsorption was carried out on a reciprocating shaker at a rate of 80 rpm at 25 °C. The solutions before and after adsorption were quantified for the amounts of Cu^{2+} ions by HITACHI 180-80 atomic absorption spectroscope (AAS). The Cu^{2+} adsorption capacities of the gels (q, in mmol/g) were calculated according to the equation given below:

$$q = \frac{(c_0 - c_e)V}{m_{dry}} \quad (1)$$

where c_0 and c_e are the initial and final concentrations (mmol/L) of Cu^{2+} ions in the testing solution, V is the volume of the testing solution (L), and m_{dry} is the dry weight of the gel (g).

The effects of OEGMA/VDT ratio, contact time, and initial pH of the solution on adsorption were carried out at initial Cu^{2+} ion concentration of 75 mmol/L. In the experiment of pH effect, the initial pH of the testing solutions was set from 2.0 to 7.0 in case that precipitation of Cu^{2+} ions happened when the pH was higher than 7.0. To investigate the influence of counterion on the adsorption capacities of hydrogels, copper sulfate, copper nitrate and copper chloride solutions with the same concentration as that of copper perchlorate were made for adsorption capability test. To investigate the adsorption isotherm of Cu^{2+} ions, swollen hydrogels were immersed in centrifuge tubes containing copper ion solutions with different initial concentrations, ranging from 5 to 125 mmol/L, until adsorption equilibrium was achieved.

2.6. Evaluation of reusable adsorption

The Cu^{2+}-adsorbed hydrogels were rinsed with 2 mL of 1 M HCl solution for 1 h to elute the adsorbate. Then they were placed in distilled water for a week to reach swelling equilibrium and were subjected to a second-time adsorption. In the same way, consecutive adsorption–desorption cycles were repeated six times by using

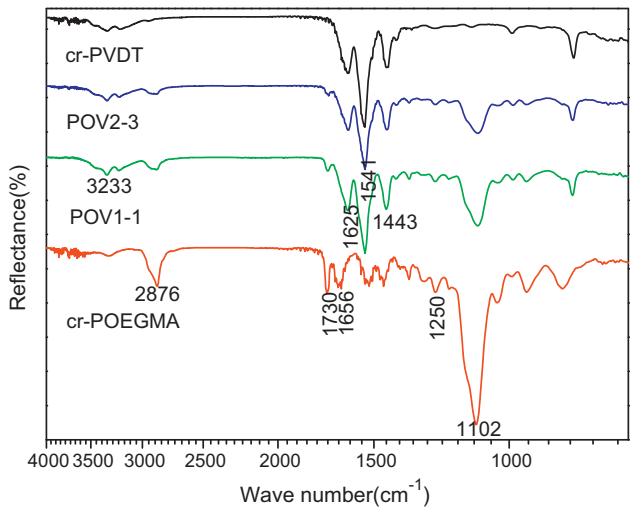

Fig. 2. ATR-FTIR spectra of cr-POEGMA, POV1-1, POV2-3 and cr-PVDT samples.

the same hydrogels so that the reusable adsorption could be determined.

3. Results and discussion

3.1. Characterization of hydrogels

The FTIR spectra of four representative hydrogel samples are shown in Fig. 2. The cr-POEGMA, POV1-1 and POV2-3 display the characteristic absorption of POEGMA: stretching vibrations of C=O and C—O—C at 1730 and 1250, 1102 cm^{-1}, respectively. The two bands locating at 1656 and 1541 cm^{-1} are attributed to the stretching vibration of C=O and the bending vibration of N—H in MBAA. The absorption bands at 3233, 2876 and 1625 cm^{-1} that are separately assigned to the stretching vibrations of N—H, C—H, and C=N in VDT [27] can all be found in cr-PVDT, POV1-1 and POV2-3. These characteristic peaks confirm the formation of P(OEGMA-co-VDT) hydrogels via photopolymerization.

3.2. Equilibrium water content (EWC) of hydrogels

The EWCs of P(OEGMA-co-VDT) hydrogels measured at room temperature are shown in Table 1. Herein, only the effect of OEGMA/VDT ratio on the EWC of the hydrogels was examined at fixed initial monomer concentration and crosslinker content. It is observed that the EWCs of the gels decrease with an increment in VDT proportion. Since 4,6-diaminotriazine (DAT) residues in neutral aqueous solution are prone to form intermolecular hydrogen bondings [28], more compact network results at higher DAT ratio, which restrains water from diffusing into the gel to a larger extent. Notably, copolymerization of hydrophilic monomer OEGMA can improve the water adsorption of hydrogels. With increasing OEGMA/VDT ratios to 3/2 and 2/1, the EWCs of the gels obtained are increased by 19% and 37%, respectively, comparing with that of cr-PVDT, 70.5%.

3.3. Mechanical properties of hydrogels

Adequate mechanical strength of a hydrogel is essential for its practical application. In this study, the mechanical properties of hydrogels with different compositions were tested and the results are demonstrated in Table 1. Obviously, the mechanical properties of hydrogels strongly depend on the content of VDT. The tensile strength, Young's modulus and compression strength all exhibit remarkable increase upon raising the content of VDT. While the VDT/OEGMA ratio is increased to 3/2, the tensile strength goes up dramatically. In comparison, POV1-2 shows the highest strengths (314 kPa tensile strength, 234 kPa modulus and 5.963 MPa compression strength). Bending to any direction cannot destroy the POV hydrogels. The self-hydrogen bonding effect among VDT moieties induces the form of rigid six-membered ring structure, which contributes to the strengthening of hydrogels [28], as revealed in our previous work [29]. After Cu^{2+} ions adsorption, the mechanical properties of the hydrogels show no weakening (Fig. 3). Take Cu^{2+}-adsorbed POV2-3 hydrogel for example, twisting, knotting and elongation cannot damage it (Fig. 3). Moreover, the hydrogel is able to withstand a large strain of compression and can recover to its original shape after the load is removed.

3.4. Copper ion adsorption assay

3.4.1. Effect of OEGMA/VDT ratio

Fig. 4 exhibits a parabolic variation of copper ion adsorption as a function of OEGMA/VDT ratio. In the case of cr-POEGMA gel, there are no typical groups that can bind Cu^{2+} strongly. So the small amount of Cu^{2+} adsorbed onto the hydrogel was mostly caused by physical adsorption onto the porous material. As the content of VDT in the hydrogel increases, the adsorption capacity increases until a maximum value of 1.25 mmol/g is achieved onto POV3-2. With further increasing VDT ratio, the adsorption ability starts to drop. For POV hydrogels that adsorb Cu^{2+} ions, two main factors should be taken into account: chelating groups and hydrophobicity. The increase of the adsorption onto POV gel (from POV2-1 to POV3-2) is due to the increment in the amino groups which can serve as chelating sites for binding Cu^{2+} ions by forming complexes. The negative effect of hydrophobicity is negligible because the hydrogels with these formulations are highly hydrophilic, as can be seen from the EWCs in Table 1. However, Further increasing VDT ratios results in the increase in the hydrophobicity

Table 1
EWCs and mechanical properties of hydrogels.

Hydrogel	EWC (%)	Tensile properties			Compression	
		Tensile strength (kPa)	Elongation at break (%)	Young's Modulus (kPa)	Stress (kPa)	Fracture strain (%)
cr-POEGMA	95.8 ± 1.1	–[a]	–[a]	–[a]	–[a]	–[a]
POV2-1	90.1 ± 1.1	–[a]	–[a]	–[a]	–[a]	–[a]
POV3-2	89.5 ± 0.7	9.3 ± 1.5	28.8 ± 1.5	32.6 ± 7.1	100.0 ± 10.0	12.1 ± 2.0
POV1-1	83.6 ± 1.3	42.0 ± 12.0	36.6 ± 1.4	115.5 ± 37.0	2320.0 ± 395.9	63.1 ± 6.3
POV2-3	77.4 ± 2.6	260.7 ± 19.0	140.1 ± 8.0	187.0 ± 23.5	4290.0 ± 174.4	87.5 ± 2.1
POV1-2	75.9 ± 1.3	314.3 ± 33.7	134.9 ± 30.0	234.5 ± 12.7	5963.3 ± 319.7	96.0 ± 7.6
cr-PVDT	70.5 ± 3.5	–[a]	–[a]	–[a]	–[a]	–[a]

[a] Measures for cr-POEGMA, POV2-1, and cr-PVDT were not available due to the weak strength.

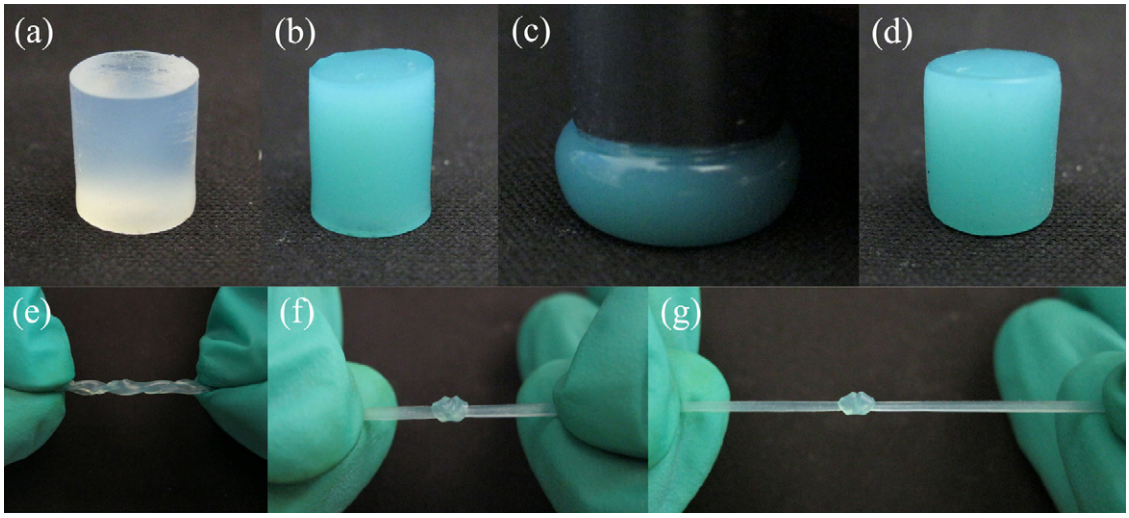

Fig. 3. Photographs of POV2-3 hydrogel before and after Cu^{2+} ions adsorption and the ability of Cu^{2+}-adsorbed hydrogel to withstand compressing, twisting and knotting. (a) POV2-3 hydrogel cylinder without Cu^{2+} adsorption; (b) Cu^{2+}-adsorbed hydrogel before compression; (c) perpendicular compression; (d) recovery after compression was removed; (e) Cu^{2+}-adsorbed hydrogel under twisting; (f) knotting; (g) knotting followed by elongation.

of polymer network. In this case, the gels shrank, accordingly reducing the specific surface area for the metal ions to deposit. On the other hand, more compact network resulting from higher VDT feed ratio restrains the exposure of amino moieties toward copper ions. Consequently, although the amount of amino groups increases, the positive effect of amino groups on adsorption is significantly limited.

3.4.2. Effect of contact time

Fig. 5 shows the effect of contact time on Cu^{2+} ions adsorption onto POV2-3 hydrogel. The adsorption capacity shows a significant increase with time during the first 30 min, and then slows down and reaches equilibrium within about 60 min, suggesting saturated adsorption. The mechanism of the adsorption kinetics is evaluated in the form of two semiempirical kinetics models: the pseudo-first-order and pseudo-second-order models. The pseudo-first-order equation [10] can be expressed as:

$$\log(q_e - q_t) = \log\ q_e - \frac{k_1}{2.303}t \tag{2}$$

where q_e and q_t (mmol/g) are the adsorption capacity of Cu^{2+} ions at equilibrium and time t (min), respectively. k_1 is the pseudo-first-order kinetic constant (min^{-1}). By fitting $\log(q_e - q_t)$ versus t linearly(Fig. 6A), the values of kinetic constant k_1 and calculated q_e (q_{ec}) can be determined from the slope of the plot and the antilogarithm of the y-intercept, respectively.

On the other hand, the pseudo-second-order model [6] can be written in the form:

$$\frac{t}{q_t} = \frac{1}{k_2 q_e^2} + \frac{t}{q_e} \tag{3}$$

where k_2 is the pseudo-second-order kinetic constant (g/mmol min). By using the data in Fig. 5, the plots of t/q_t as a function of the time t can be constructed as shown in Fig. 6B. The values of calculated q_e (q_{ec}) and the constant k_2 can be obtained

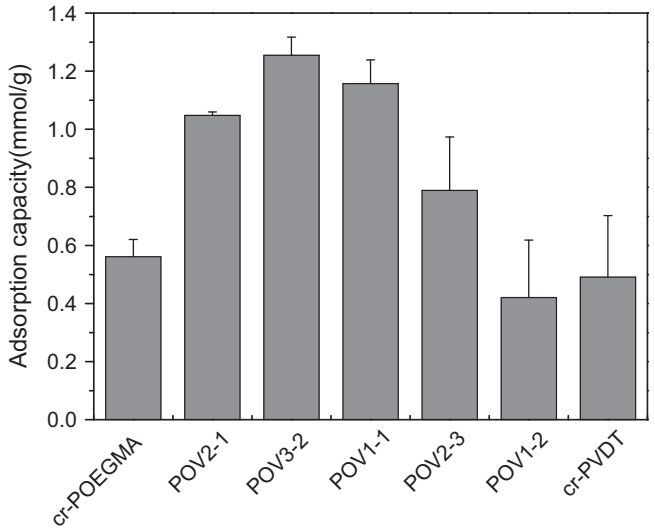

Fig. 4. Adsorption capacity of hydrogels with varied OEGMA/VDT ratios.

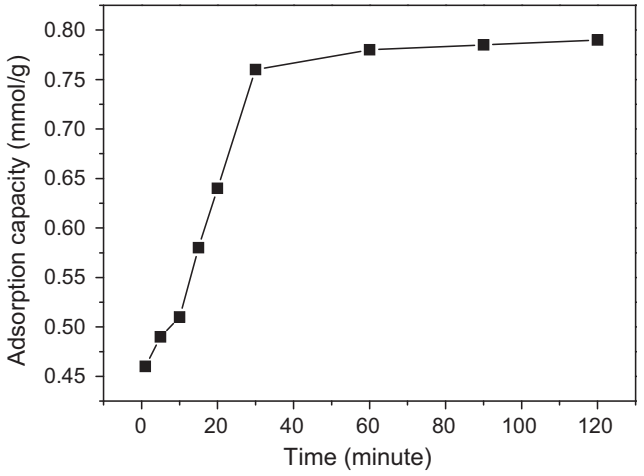

Fig. 5. Effect of contact time on the adsorption of Cu^{2+} ions onto POV2-3 hydrogel.

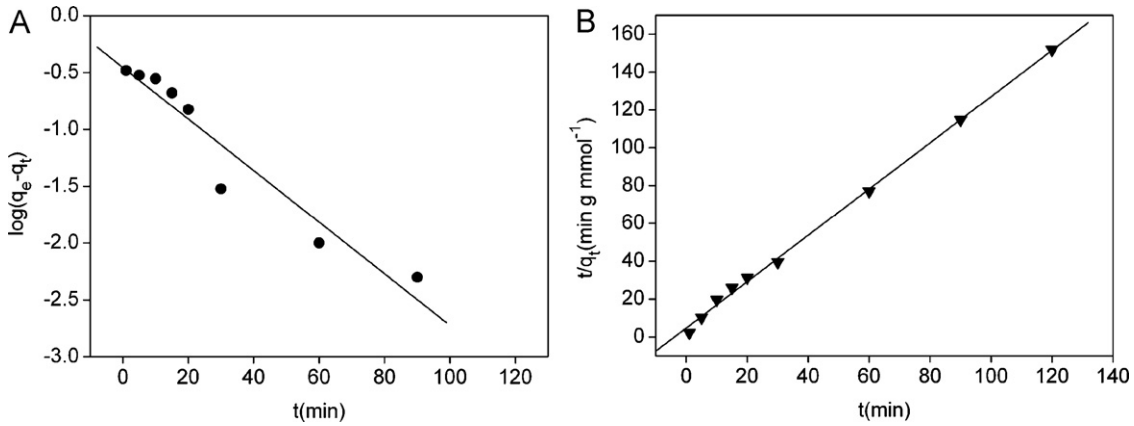

Fig. 6. Adsorption kinetics of Cu^{2+} ions onto POV2-3 hydrogel based on pseudo-first-order kinetic model (A) and pseudo-second-order kinetic model (B).

from the slope values of the linear plots and the *y*-interception values, respectively.

The values of k_1, k_2 and q_{ec} as well as the correlation coefficient (r^2) are summarized in Table S2. The validity of each model can be validated by comparing the values of correlation coefficient (r^2). On the basis of the values of r^2 in Table S2, it can be concluded that the pseudo-second-order model is more suitable for describing the adsorption of Cu^{2+} ions onto the hydrogels than the pseudo-first-order model. Moreover, the q_{ec2} calculated from the pseudo-second-order model is more approximate to the experimental values of q_e, but the value of q_{ec1} is far away from it. So the pseudo-first-order model is unsuitable for describing the adsorption process.

3.4.3. Effect of initial pH

Fig. S1 shows the effect of pH values of solution on the adsorption capacity of the hydrogels. The initial concentration of copper ion was the same as that in the experiment of contact time effect, and the adsorption time was set at 60 min, i.e. the adsorption equilibrium time as determined in Fig. 5. As seen from Fig. S1, the adsorption capacity increases significantly along with the increase in pH values, and reaches a maximum at pH 7. It can be explained by the fact that most of the amine groups are protonated in the acidic environment. Under this condition, the electrostatic repulsion happens between Cu^{2+} ions and the protonated amines so that there are fewer amine groups available to capture Cu^{2+} ions. The lower the pH value, the stronger the repulsive force. So at the lowest pH, only small amounts of Cu^{2+} ions are adsorbed onto the hydrogels.

3.4.4. Effect of counter ion

To demonstrate the versatility of the hydrogels, different types of copper salts (copper sulfate, copper nitrate and copper chloride) were chosen for adsorption experiments in comparison with copper perchlorate. From the results shown in Fig. S2, one can see that the effect of counter ions on the adsorption of Cu^{2+} ions onto the same POV2-3 hydrogel is apparent. The adsorption capacities are in the descending order: $CuSO_4 > Cu(ClO_4)_2 > Cu(NO_3)_2 > CuCl_2$. And there is no significant difference in adsorption capacities between $CuSO_4$ and $Cu(ClO_4)_2$. Since the effect of counterion on adsorption is complicated, here we cannot give a clear explanation. It is possible that ClO_4^- and SO_4^{2-} can stabilize the Cu^{2+} ion adsorption on the concentrated amino sites as well as on the unfavorable site by coadsorption with copper ions [30]. The reason for the reduction trend of $Cu(NO_3)_2$ and $CuCl_2$ species remains unknown using present method and needs to be further investigated in the future. Nevertheless, the results demonstrate that Cu^{2+} ions could be adsorbed on the hydrogels in the presence of different counter ions.

3.4.5. Adsorption isotherms

The adsorption capacities of Cu^{2+} ions onto POV2-3 hydrogels immersing in different concentrations of copper ion are shown in Fig. 7. The results indicate that the adsorption capacity increases with an increment in initial concentration of Cu^{2+} ions. The amounts of copper ion adsorbed are increased remarkably at lower concentration due to the adequate adsorption sites and the increase in number of Cu^{2+} ion transported from the bulk solution to the hydrogel. However, the adsorption capacity levels off at 75 mmol/L, indicating that the adsorption reaches a saturation due to the limited number of the adsorption sites. To explore the adsorption mechanism, two adsorption isotherm models are used to describe how adsorbates interact with adsorbents: Langmuir and Freundlich isotherms.

The Langmuir isotherm model assumes that the adsorbed layer is a homogeneous, flat surface that has only one molecule in thickness, and that each adsorptive site can be occupied by only one adsorbate molecule. Mathematically, it can be written as follows [10,31]:

$$\frac{C_e}{q_e} = \frac{1}{K_L q_m} + \frac{C_e}{q_m} \quad (4)$$

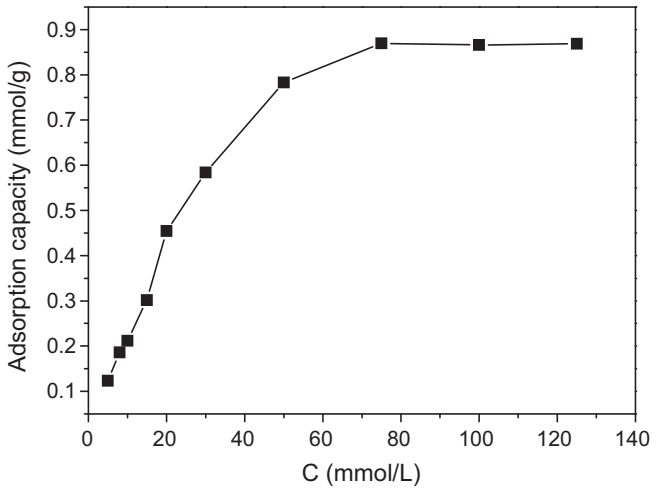

Fig. 7. Effect of initial concentration of Cu^{2+} ions on the adsorption capacity of POV2-3 hydrogel.

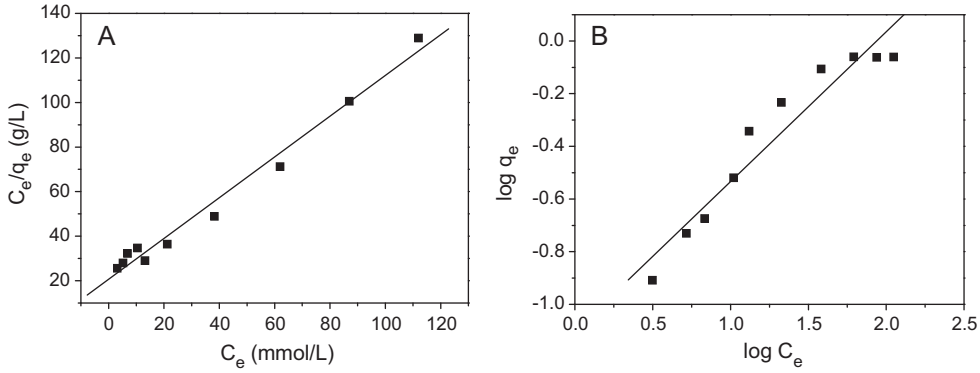

Fig. 8. Langmuir (A) and Freundlich (B) adsorption isotherms for the adsorption of Cu^{2+} ions onto POV2-3 hydrogels.

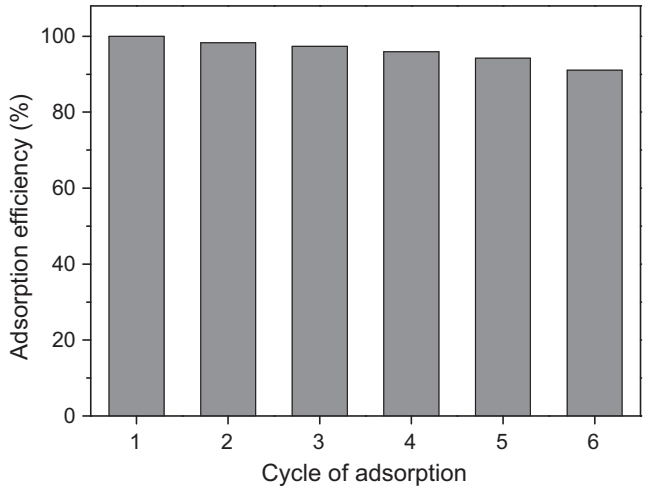

Fig. 9. Effect of adsorption cycle on adsorption capacity of POV2-3 hydrogel.

where C_e is the equilibrium Cu^{2+} ion concentration in the test solution (mmol/L), q_e represents the equilibrium adsorption amount of Cu^{2+} ions onto hydrogels (mmol/g), q_m is the maximal adsorption capacities of Cu^{2+} ions onto hydrogels (mmol/g), and K_L is the Langmuir constant ($L\,mmol^{-1}$). By linearly plotting C_e/q_e as the function of C_e, the values of K_L and q_m can be obtained from the y-intercept and the slope of the plot. The values of these parameters, as analyzed from the plots shown in Fig. 8A, are summarized in Table S3.

The experimental data can also be analyzed by Freundlich model, which is applicable to nonideal adsorption on heterogeneous surfaces and multilayer sorption. The model is expressed as follows [31,32]:

$$\log\ q_e = \log K_F + \frac{1}{n}\log C_e \quad (5)$$

where K_F and n are the Freundlich constants representing the adsorption capacity (mmol/g) and the adsorption intensity (dimensionless), respectively. The values of K_F and n are taken as the antilogarithm of the y-intercept and reciprocal of the slope. The values of the parameters analyzed from the plots shown in Fig. 8B are also summarized in Table S3.

It is clear that the Langmuir isotherm model gives the better fit than the Freundlich model, as indicated by comparison of the correlation coefficient (r^2). The result suggests that the adsorption of copper ions onto the hydrogels follows a phenomenon mostly represented by the Langmuir model. In another word, the surface of the hydrogel may be homogeneous and it is possible that a monolayer of Cu is adsorbed on the hydrogel [31]. And from the value of q_m, the maximal adsorption capacity of POV2-3 hydrogel is calculated to be 1.093 mmol/g.

3.5. Adsorption/desorption cycles of reusable hydrogels

A promising adsorbent is required to have not only high adsorption capacity but also regeneration ability for recycling use, which is energy saving, meeting the demand of low carbon economy. In this work, reproducible adsorption/desorption of copper ions onto the hydrogels was inspected. We found that Cu^{2+} ions could be effectively eluted from hydrogels by using 1 M HCl solution and the desorption efficiency reached up to 99%. Fig. 9 shows that after six adsorption–desorption cycles, in spite of slight decline, over 90% adsorption capacity is still retained. It is noted that the mechanical strength of hydrogels did not show any evident distinction after six cycles, manifesting their durability for repeated use. From Fig. 10,

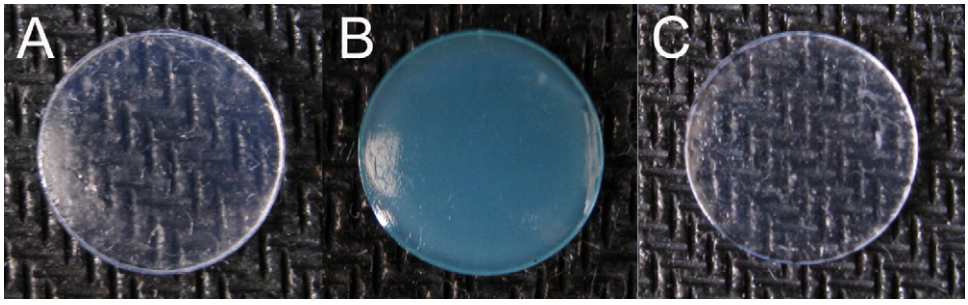

Fig. 10. Photographs of POV2-3 hydrogel before adsorption (A), after six-time adsorption (B) and desorption (C).

we can see a good reproducibility of hydrogel in color and shape after six cycles.

4. Conclusions

Mechanically robust OEGMA/VDT copolymer hydrogels synthesized by photoinitiated polymerization exhibited several MPa compressive stresses at an appropriate monomer ratio, ensuring easy handling in practical application. With the increase in the weight ratio of VDT, the adsorption capacity increased at first and then decreased as the result of mutual restriction between the increase in number of chelating sites for Cu^{2+} ions and increased compactness of network. The adsorption of Cu^{2+} ions onto the hydrogels reached equilibrium within about 60 min. In the pH range 2–7, higher pH values in the solution resulted in better adsorption performance of Cu^{2+} ions onto the hydrogels. The experimental adsorption data could be better fitted by Langmuir isotherm model rather than Freundlich model, and the maximal adsorption capacity was calculated to be 1.1 mmol/g. Copper ions could be desorbed from the hydrogels by using 1 M HCl aqueous solution and the desorption efficiency could reach up to 99%. After six adsorption–desorption cycles, the adsorption capacity could be maintained above 90% with no significant loss in mechanical properties.

Acknowledgment

The authors gratefully acknowledge the support for this work from the National Natural Science Foundation of China (Grants 30770587, 50973082).

Appendix A. Supplementary data

Supplementary data associated with this article can be found, in the online version, at doi:10.1016/j.jhazmat.2012.01.092.

References

[1] S. Veli, B. Alyuz, Adsorption of copper and zinc from aqueous solution by using natural clay, J. Hazard. Mater. 149 (2007) 226–233.
[2] M.C. Basso, E.G. Cerrella, A.L. Cukierman, Activated carbons developed from a rapidly renewable biosource for removal of cadmium(II) and nickel(II) from dilute aqueous solutions, Ind. Eng. Chem. Res. 41 (2002) 180–189.
[3] S. Gomez-Salazar, J.S. Lee, J.C. Heydweiller, L.L.S. Tavlarides, Analysis of cadmium adsorption on novel organo-ceramic adsorbents with a thiol functionality, Ind. Eng. Chem. Res. 42 (2003) 3403–3412.
[4] C.P. Huang, Y.C. Chung, M.R. Liou, Adsorption of Cu(II) and Ni(II) by palletized biopolymer, J. Hazard. Mater. 45 (1996) 265–277.
[5] M. Monier, D.M. Ayad, A.A. Sarhan, Adsorption of Cu(II), Hg(II), and Ni(II) ions by modified natural wool chelating fibers, J. Hazard. Mater. 176 (2010) 348–355.
[6] X.W. Liu, Q.Y. Hu, Z. Fang, X.J. Zhang, B.B. Zhang, Magnetic chitosan nanocomposites: a useful recyclable tool for heavy metal ion removal, Langmuir 25 (2009) 3–8.
[7] C.W. Cheung, J.F. Porter, G. McKay, Removal of Cu(II) and Zn(II) ions by sorption onto bone char using batch agitation, Langmuir 18 (2002) 650–656.
[8] K.F. Lam, X. Chen, C.M. Fong, K.L. Yeung, Selective mesoporous adsorbents for Ag^{+}/Cu^{2+} separation, Chem. Commun. 17 (2008) 2034–3036.
[9] V. Manu, H.M. Mody, H.C. Bajaj, R.V. Jasra, Adsorption of Cu^{2+} on amino functionalized silica gel with different loading, Ind. Eng. Chem. Res. 48 (2009) 8954–8960.
[10] P. Kampalanonwat, P. Supaphol, Preparation and adsorption behavior of aminated electrospun polyacrylonitrile nanofiber mats for heavy metal ion removal, ACS Appl. Mater. Interface 2 (2010) 3619–3627.
[11] S.B. Deng, R.B. Bai, J.P. Chen, Aminated polyacrylonitrile fibers for lead and copper removal, Langmuir 19 (2003) 5058–5064.
[12] A. Demirbas, E. Pehlivan, F. Gode, T. Altun, G. Arslan, Adsorption of Cu(II), Zn(II), Ni(II), Pb(II), and Cd(II) from aqueous solution on Amberlite IR-120 synthetic resin, J. Colloid Interface Sci. 282 (2005) 20–25.
[13] S. Rengaraj, S.H. Moon, Kinetics of adsorption of Co(II) removal from water and wastewater by ion exchange resins, Water Res. 36 (2002) 1783–1793.
[14] J.P. Chen, L. Hong, S.N. Wu, L. Wang, Elucidation of interactions between metal ions and Ca alginate-based ion-exchange resin by spectroscopic analysis and modeling simulation, Langmuir 18 (2002) 9413–9421.
[15] L.F. Chen, H.W. Liang, Y. Lu, C.H. Cui, S.H. Yu, Synthesis of an attapulgite clay@carbon nanocomposite adsorbent by a hydrothermal carbonization process and their application in the removal of toxic metal ions from water, Langmuir 27 (2011) 8998–9004.
[16] J. Hu, I.M.C. Lo, G.H. Chen, Fast removal and recovery of Cr(VI) using surface-modified jacobsite ($MnFe_2O_4$) nanoparticles, Langmuir 21 (2005) 11173–11179.
[17] M. Arias, C. Pérez-Novo, F. Osorio, E. López, B. Soto, Adsorption and desorption of copper and zinc in the surface layer of acid soils, J. Colloid Interface Sci. 288 (2005) 21–29.
[18] M.K. Doula, A. Ioannou, The effect of electrolyte anion on Cu adsorption–desorption by clinoptilolite, Micropor. Mesopor. Mater. 58 (2003) 115–130.
[19] J.P. Chen, L. Yang, Study of a heavy metal biosorption onto raw and chemically modified *sargassum* sp. via spectroscopic and modeling analysis, Langmuir 22 (2006) 8906–8914.
[20] V. Bekiari, M. Sotiropoulou, G. Bokias, P. Lianos, Use of poly(N,N-dimethylacrylamide-co-sodium acrylate) hydrogel to extract cationic dyes and metals from water, Colloids Surf. A 312 (2008) 214–218.
[21] H. Kasgoz, S. Ozgumus, M. Orbay, Modified polyacrylamide hydrogels and their application in removal of heavy metal ions, Polymer 44 (2003) 1785–1793.
[22] A.E. Ali, H.A. Shawky, H.A.A.E. Rehim, E.A. Hegazy, Synthesis and characterization of PVP/AAc copolymer hydrogel and its applications in the removal of heavy metals from aqueous solution, Eur. Polym. J. 39 (2003) 2337–2344.
[23] T. Trakulsujaritchok, N. Noiphom, N. Tangtreamjitmun, R. Saeeng, Adsorptive features of poly(glycidyl methacrylateco-hydroxyethyl methacrylate): effect of porogen formulation on heavy metal ion adsorption, J. Mater. Sci. 46 (2011) 5350–5362.
[24] I. Katime, E. Rodriguez, Adsorption of metal ions and swelling properties of poly(acrylic acid-co-itaconic acid) hydrogels, J. Macromol. Sci.: Pure Appl. Chem. A 38 (5–6) (2001) 543–558.
[25] A.S. Hoffman, Hydrogels for biomedical applications, Adv. Drug Deliv. Rev. 43 (2002) 3–12.
[26] S. Cavus, G. Gurdag, K. Sozgen, M.A. Gurkaynak, The preparation and characterization of poly(acrylic acid-co-methacrylamide) gel and its use in the non-competitive heavy metal removal, Polym. Adv. Technol. 20 (2009) 165–172.
[27] L. Tang, Y. Yang, T. Bai, W.G. Liu, Robust MeO_2MA/vinyl-4,6-diamino-1,3,5-triazine copolymer hydrogels-mediated reverse gene transfection and thermo-induced cell detachment, Biomaterials 32 (2011) 1943–1949.
[28] K.E. Maly, C. Dauphin, J.D. Wuest, Self-assembly of columnar mesophases from diaminotriazines, J. Mater. Chem. 16 (2006) 4695–4700.
[29] L. Tang, W.G. Liu, G.P. Liu, High-strength hydrogels with integrated functions of H-bonding and thermoresponsive surface-mediated reverse transfection and cell detachment, Adv. Mater. 22 (2010) 2652–2656.
[30] K.F. Lam, X.Q. Chen, G. McKay, K.L. Yeung, Anion effect on Cu^{2+} adsorption on NH_2-MCM-41, Ind. Eng. Chem. Res. 47 (2008) 9376–9383.
[31] M.M. Bekheit, N. Nawar, A.W. Addison, D.A. Abdel-Latif, M. Monier, Preparation and characterization of chitosan-grafted-poly(2-amino-4,5-pentamethylene-thiophene-3-carboxylic acid N′-acryloyl-hydrazide) chelating resin for removal of Cu(II), Co(II) and Ni(II) metal ions from aqueous solutions, Int. J. Biol. Macromol. 48 (2011) 558–565.
[32] H. Chen, A.Q. Wang, Adsorption characteristics of Cu(II) from aqueous solution onto poly(acrylamide)/attapulgite composite, J. Hazard. Mater. 165 (2009) 223–231.